

Dark Energy Interacting with Dark Matter in Classical Einstein and Loop Quantum Cosmology

Song Li and Yongge Ma

Department of Physics, Beijing Normal University, Beijing 100875, P. R. China

The cosmological model of dark energy interacting with cold dark matter without coupling to the baryonic matter, is studied in the background of both classical Einstein and loop quantum cosmology. We consider two types of interacting models. In the former model, the interaction is a linear combination of the densities of two dark sectors, while in the latter model, the interaction with a constant transfer rate depends only on the density of cold dark matter. It is shown that the dynamical results in loop quantum cosmology are different from those in classical Einstein cosmology for both two kinds of interacting models. Moreover, the form of the interaction affects significantly the dynamical results in both kinds of cosmology.

PACS numbers: 98.80.Cq, 98.80.-k

I. INTRODUCTION

Recently, the discovery of the acceleration of cosmological expansion at present epoch has been the most principal achievement of observational cosmology. Numerous cosmological observations, such as Type Ia Supernovae (SNIa) [1], Cosmic Microwave Background Radiation (CMBR) [2] and Large Scale Structure [3], strongly suggest that the universe is spatially flat with about 4% ordinary baryonic matter, 20% dark matter and 76% dark energy. The accelerated expansion of the present universe is attributed to the dominant component of the universe, dark energy, which has a large negative pressure but not cluster. In fact, it has not been detected directly and there is no justification for assuming that dark energy resembles known forms of matter or energy. A large body of recent work has focussed on understanding the nature of dark energy. However, the physical origin of dark energy as well as its nature remain enigmatic at present.

The simplest model of dark energy is the cosmological constant Λ [4], whose energy density remains constant with time $\rho_\Lambda = \Lambda/8\pi G$ (natural units $c = \hbar = 1$ is used throughout the paper) and whose equation of state (defined as the ratio of pressure to energy density) remains $w = -1$ as the universe evolves. Unfortunately, the model is burdened with the well-known cosmological constant problems, namely the fine-tuning problem: why is the energy of the vacuum so much smaller than its estimation? and the cosmic coincidence problem: why is the dark energy density approximately equal to the matter density today? These problems have led many researchers to try different approaches to the dark energy issue. A possible method is to assume the equation of state (EoS) w is a dynamical variable, and thus the dynamical scenario of dark energy is investigated. The most popular model among them is dubbed quintessence [5]. Besides, other scalar-field dark energy models have been studied, including phantom [6], tachyon [7], quintom [8], ghost condensates [9], etc. Also, there are other candidates, for example, Chaplygin gas which attempt to unify dark energy and dark matter [10], braneworld model [11] and 5-dimensional gravity model [12] which explain the acceleration through the assumption that spacetime has five dimensions instead of the usual four. In addition, since the cosmological scaling solution (i.e., the energy densities of dark energy and cold dark matter remain proportional) could probably alleviate the coincidence problem, interacting dark energy models are also proposed [13].

As we all know, observations at the level of the solar system severely constrain non-gravitational interactions of baryons, namely, non-minimal coupling between dark energy and ordinary matter fluids is strongly restricted by the experimental tests in the solar systems [14], we therefore neglect this possibility. However, since the nature of dark sectors remains unknown, it is possible to have non-gravitational interactions between dark energy and dark matter. So we focus on dark energy interacting with dark matter alone.

Actually, many dark energy models are considered in the framework of classical Einstein cosmology. However, an outstanding problem in classical Einstein cosmology is the big bang singularity which is expected to be solved by quantum gravity. As a background independent quantization of general relativity, loop quantum gravity (LQG) is one of the best candidate theories of quantum gravity [15]. It has been applied in cosmology to analyze our universe, known as Loop Quantum Cosmology (LQC) [16]. In LQC, non-perturbative effects lead to $-\rho^2/\rho_c$ corrections to the standard Friedmann equation and thus allow us the possibility of resolving any past and future singularities [16, 17]. The modification becomes important when energy density of the universe becomes to be the same order of a critical density ρ_c . When the correction term $-\rho^2/\rho_c$ dominates during the evolution of our universe, it will cause the quantum bounce and hence avoid the singularity. Recently, more and more researchers have taken their attention to LQC for the appealing features: avoidance of various singularities [18], inflation in LQC [19], large scale effect [20] and so on. Concretely, some dark energy models are investigated in the background of LQC, such as phantom [21],

coupling phantom [22], quintom and hessence [23], interacting dark energy model [24], etc.

In this paper, we study the dynamical evolution of two classes of interacting dark energy models in classical Einstein and Loop Quantum Cosmology. Here some questions naturally arise as follows. Can these models alleviate the coincidence problem in classical Einstein cosmology? Are there scaling solutions arising from the effect of loop quantum cosmology? Can the future singularities be resolved in LQC? By our analysis, it turns out that in the former model, there are two attractors in classical Einstein cosmology and LQC. One is an accelerated scaling solution and the other is a baryon dominant solution. However, in the latter model, there exists one attractor in classical Einstein cosmology, which is a dark energy dominated solution rather than a scaling solution, whereas in LQC all fixed points are unstable. Thus, there exists no scaling solution in the latter case, namely, this kind of interacting dark energy model can not be regarded as a candidate to alleviate the coincidence problem. Also, we find that dynamical results in LQC are different from those in classical Einstein cosmology for both two kinds of interacting models. Our universe finally enters an oscillating phase in LQC. Moreover, the oscillating frequencies are significantly different for varied parameters of models. These results are different from the those obtained in classical Einstein cosmology. Thus, LQC allow us the possibility of resolving future singularities. Hence, the quantum gravity effect may be manifested in large scale in the interacting dark energy models.

In Sec. II, we study dynamical properties for the general case in classical Einstein cosmology and LQC. Then the dynamical results of two types of interacting models are respectively studied in Secs. III and IV. In Sec. V, the numerical results are presented. Finally, the conclusions are summarized in Sec. VI.

II. INTERACTING DARK ENERGY MODEL IN CLASSICAL EINSTEIN COSMOLOGY AND LQC

For a spatially flat universe, the total energy conservation equation is

$$\dot{\rho} + 3H(\rho + p) = 0, \quad (1)$$

where H is the Hubble parameter, ρ is the total energy density and p is the total pressure of the background fluid.

In our scenario, the universe contains dark energy, cold dark matter and baryonic matter. Moreover, the two dark sectors interact through the interaction term Q and the baryonic matter only interacts gravitationally with the dark sectors. Then the energy conservation equation is written as

$$\dot{\rho}_b + 3H\rho_b = 0, \quad (2)$$

$$\dot{\rho}_m + 3H\rho_m = Q, \quad (3)$$

$$\dot{\rho}_d + 3H(1 + w_d)\rho_d = -Q, \quad (4)$$

where the subscripts b , m and d respectively denote baryonic matter, cold dark matter and dark energy. In this paper, we consider the simplest case of dark energy with constant equation of state $w_d = p_d/\rho_d$ [25], although the equation of state for dark energy could also be dynamic. Thus, Q denotes the energy density exchange in the dark sectors and the sign of Q determines the direction of energy transfer. A positive Q corresponds to the transfer of energy from dark energy to dark matter, while a negative Q represents the other way round. Due to the unknown nature of dark sectors, there is as yet no basis in fundamental theory for a special coupling between two dark sectors. So the interaction term Q discussed currently have to be chosen in a phenomenological way [26]. Since there is no clear consensus on the form of the coupling, different versions, that arise from a variety of motivations, coexist in the literature.

A. Classical Einstein Cosmology

In classical Einstein cosmology, the Friedmann equation is given by

$$H^2 = \frac{\kappa^2}{3}\rho = \frac{\kappa^2}{3}(\rho_d + \rho_m + \rho_b), \quad (5)$$

where $\kappa^2 \equiv 8\pi G$. Then differentiating the above equation with respect to cosmic time t and using the total energy conservation equation, we can get the Raychaudhuri equation

$$\begin{aligned} \dot{H} &= -\frac{\kappa^2}{2}(\rho + p) \\ &= -\frac{\kappa^2}{2}((1 + w_d)\rho_d + \rho_m + \rho_b). \end{aligned} \quad (6)$$

To analyze the evolution of the dynamical system, we introduce the following set of dimensionless variables:

$$x \equiv \frac{\kappa^2 \rho_d}{3H^2}, \quad y \equiv \frac{\kappa^2 \rho_m}{3H^2}, \quad z \equiv \frac{\kappa^2 \rho_b}{3H^2}, \quad u \equiv \frac{\kappa^2 Q}{3H^3}. \quad (7)$$

Accordingly, the Friedmann constraint is

$$x + y + z = 1, \quad (8)$$

and Eqs. (5) and (6) can be written as

$$-\frac{\dot{H}}{H^2} = \frac{3}{2}(1 + w_d x). \quad (9)$$

Furthermore, using these variables, the EoS of the total cosmic fluid is given by

$$w = \frac{p}{\rho} = \frac{w_d x}{x + y + z} = w_d x. \quad (10)$$

Then, inserting the expression (7) into Eqs.(2)-(6), we can obtain the following autonomous system:

$$x' = -3w_d x(1 - x) - u, \quad (11)$$

$$y' = 3w_d x y + u, \quad (12)$$

$$z' = 3w_d x z, \quad (13)$$

where the prime denotes a derivative with respect to $N \equiv \ln a$. We set the current scale factor by $a_0 = 1$, then the current value of N reads $N_0 = 0$. Setting $x' = y' = z' = 0$, we can find the general solution of the critical points (x_*, y_*, z_*) of the autonomous system (11)-(13) as the type of $(x_* = 0, u_* = 0)$ and $(x_* + y_* = 1, z_* = 0)$.

B. Loop Quantum Cosmology

Due to the quantum effects in LQC, we consider effective Friedmann equation with correction of the form [16]

$$H^2 = \frac{\kappa^2}{3} \rho \left(1 - \frac{\rho}{\rho_c}\right), \quad (14)$$

where $\rho = \rho_d + \rho_m + \rho_b$, the critical density $\rho_c \equiv \frac{\sqrt{3}}{16\pi^2 \gamma^3} \rho_{pl}$ measures the loop quantum effects, ρ_{pl} is the Planck density, γ is the dimensionless Barbero-Immirzi parameter [27]. An important feature for the modified dynamics is that a ρ^2 term which is relevant in the high energy regime is included in the classical Friedmann equation. The correction term predicts a bounce when the matter energy density reaches the critical value ρ_c which is close to the Planck density. By the numerical simulation [16], it turns out that the modified Friedmann equation is valid in the whole evolutionary trajectory of the universe including the bounce. Additionally, along with the total energy conservation equation, we get

$$\begin{aligned} \dot{H} &= -\frac{\kappa^2}{2}(\rho + p)\left(1 - 2\frac{\rho}{\rho_c}\right) \\ &= -\frac{\kappa^2}{2}\left((1 + w_d)\rho_d + \rho_m + \rho_b\right)\left(1 - 2\frac{\rho_d + \rho_m + \rho_b}{\rho_c}\right). \end{aligned} \quad (15)$$

Using the dimensionless variables defined in (7), the Friedmann constraint is

$$(x + y + z)\left(1 - \frac{3H^2}{\kappa^2} \frac{x + y + z}{\rho_c}\right) = 1, \quad (16)$$

and Eqs. (14) and (15) can be written as

$$-\frac{\dot{H}}{H^2} = \frac{3}{2}(2 - x - y - z)\left(1 + \frac{w_d x}{x + y + z}\right). \quad (17)$$

Point	(x_*, y_*, z_*)	Eigenvalues	w_*
A	$(-\frac{c_1 - c_2 - w_d - x_s}{2w_d}, -\frac{c_1 - c_2 + w_d - x_s}{2w_d}, 0)$	$\lambda_1 = 3x_s,$ $\lambda_2 = \lambda_3 = -\frac{3}{2}(c_1 - c_2 - w_d - x_s)$	$-\frac{c_1 - c_2 - w_d - x_s}{2}$
B	$(-\frac{c_1 - c_2 - w_d + x_s}{2w_d}, -\frac{c_1 - c_2 + w_d + x_s}{2w_d}, 0)$	$\lambda_1 = -3x_s,$ $\lambda_2 = \lambda_3 = -\frac{3}{2}(c_1 - c_2 - w_d + x_s)$	$-\frac{c_1 - c_2 - w_d + x_s}{2}$
C	$(0, 0, 1)$	$\lambda_1 = 0,$ $\lambda_{2,3} = \frac{3}{2}(c_1 - c_2 - w_d \pm x_s)$	0

TABLE I: The properties of the critical points for the interacting model I in classical Einstein cosmology. Here, the parameter x_s is defined in Eq. (25).

Furthermore, the EoS of the total cosmic fluid reads

$$w = \frac{p}{\rho} = \frac{w_d x}{x + y + z}. \quad (18)$$

Then, Eqs.(2)-(4) combined with Eqs. (14)-(15) can be rewritten as the following autonomous system according to the expression (7),

$$x' = -3(1 + w_d)x - u + 3x(2 - x - y - z)(1 + \frac{w_d x}{x + y + z}), \quad (19)$$

$$y' = -3y + u + 3y(2 - x - y - z)(1 + \frac{w_d x}{x + y + z}), \quad (20)$$

$$z' = -3z[1 - (2 - x - y - z)(1 + \frac{w_d x}{x + y + z})]. \quad (21)$$

The type of critical points of the autonomous system (19)-(21) can be summarized as $(x_* = 0, u_* = 0)$, $(x_* + y_* = 1, z_* = 0)$ and $(x_* \neq 0, y_* = -(1 + w_d)x_*, u = -3(1 + w_d)x_*)$.

III. INTERACTING DARK ENERGY MODEL I

Let us first consider the interaction term $Q = 3H(c_1\rho_m + c_2\rho_d)$ [28, 29], where c_1 and c_2 are coupling constants. Note that this form, which was first proposed in [30], is more general than those proposed in [26, 31]. The latter can be obtained from the former by setting $c_1 = c_2 = c$, $c_1 = 0$ or $c_2 = 0$. According to Ref. [28], we assume the coupling constants c_1 and c_2 have the same sign to achieve a physically viable model.

A. Cosmological Dynamics in Classical Einstein Cosmology

In classical Einstein cosmology, the autonomous system (11)-(13) can be written as

$$x' = -3[(1 + c_2 + w_d)x + c_1y] + 3x(1 + w_d x), \quad (22)$$

$$y' = -3[(1 - c_1)y - c_2x] + 3y(1 + w_d x), \quad (23)$$

$$z' = 3w_d x z. \quad (24)$$

Furthermore, we can obtain the critical points (x_*, y_*, z_*) of the autonomous system as follows:

- **Point A:** $(-\frac{c_1 - c_2 - w_d - x_s}{2w_d}, -\frac{c_1 - c_2 + w_d - x_s}{2w_d}, 0)$,

- **Point B:** $(-\frac{c_1 - c_2 - w_d + x_s}{2w_d}, -\frac{c_1 - c_2 + w_d + x_s}{2w_d}, 0)$,

- **Point C:** $(0, 0, 1)$.

Point	(x_*, y_*, z_*)	Eigenvalues	w_*
A	$(-\frac{c_1-c_2-w_d-x_s}{2w_d}, -\frac{c_1-c_2+w_d-x_s}{2w_d}, 0)$	$\lambda_1 = 3x_s,$ $\lambda_2 = -\frac{3}{2}(c_1 - c_2 - w_d - x_s),$ $\lambda_3 = -\frac{3}{2}(2 - c_1 + c_2 + w_d + x_s)$	$-\frac{c_1-c_2-w_d-x_s}{2}$
B	$(-\frac{c_1-c_2-w_d+x_s}{2w_d}, -\frac{c_1-c_2+w_d+x_s}{2w_d}, 0)$	$\lambda_1 = -3x_s,$ $\lambda_2 = -\frac{3}{2}(c_1 - c_2 - w_d + x_s),$ $\lambda_3 = -\frac{3}{2}(2 - c_1 + c_2 + w_d - x_s)$	$-\frac{c_1-c_2-w_d+x_s}{2}$
C	$(0, 0, 1)$	$\lambda_1 = -3,$ $\lambda_{2,3} = \frac{3}{2}(c_1 - c_2 - w_d \pm x_s)$	0

TABLE II: The properties of the critical points for the interacting model I in LQC. Also, the parameter x_s is defined in Eq. (25).

Here the parameter x_s is defined by

$$x_s = \sqrt{(c_1 - c_2 - w_d)^2 + 4w_dc_1}. \quad (25)$$

To study the stability of the critical points for the autonomous system, we substitute linear perturbations $x \rightarrow x_* + \delta x$, $y \rightarrow y_* + \delta y$ and $z \rightarrow z_* + \delta z$ about the critical points into the autonomous system Eqs. (22)-(24). To first-order in the perturbations, we get the following evolution equations of the linear perturbations:

$$\delta x' = -3(c_2 + w_d - 2w_dx_*)\delta x - 3c_1\delta y, \quad (26)$$

$$\delta y' = 3(c_2 + w_dy_*)\delta x + 3(c_1 + w_dx_*)\delta y, \quad (27)$$

$$\delta z' = 3w_dz_*\delta x + 3w_dx_*\delta z. \quad (28)$$

The three eigenvalues of the coefficient matrix of Eqs. (26)-(28) determine the stability of the critical points. We list the three eigenvalues for each point in Table I. We examine the sign of the eigenvalues of points A and B and find that point A is not stable if it exists, whereas point B is stable if $0 < c_1 < -w_d$ and $0 < c_2 < c_1 - w_d - 2\sqrt{-w_dc_1}$, i.e., the critical point B is always the stable attractor solution if it exists. In addition, at point B, from the expression of the total EoS $w_* = -\frac{c_1-c_2-w_d+x_s}{2}$, the acceleration condition $w < -1/3$ shows that if

$$\begin{cases} w_d > -1/3, & 0 < c_1 < -w_d, & 0 < c_2 < (1 + 3w_d)c_1 - w_d + 1/3; \\ -2/3 < w_d < -1/3, & w_d + 2/3 < c_1 < -1/(9w_d), & 0 < c_2 < (1 + 3w_d)c_1 - w_d + 1/3; \\ w_d < -2/3, & 0 < c_1 < -1/(9w_d), & 0 < c_2 < (1 + 3w_d)c_1 - w_d + 1/3; \\ w_d < -1/3, & -1/(9w_d) < c_1 < -w_d, & 0 < c_2 < c_1 - w_d - 2\sqrt{-w_dc_1}, \end{cases} \quad (29)$$

point B is an accelerated scaling attractor where the energy densities of dark energy and cold dark matter remain proportional. Thus it may alleviate the coincidence problem. The baryon dominated point C is stable if $c_1 - c_2 - w_d < 0$ and $4w_dc_1 < 0$. This condition corresponds to $c_1 > 0$ and $c_2 > c_1 - w_d$ under the prior condition $w_d < 0$.

B. Cosmological Dynamics in LQC

We consider the autonomous system (19)-(21) in LQC. By inserting the concrete form of Q into Eqs.(19)-(21), the autonomous system can be expressed as

$$x' = -3[(1 + c_2 + w_d)x + c_1y] + 3x(2 - x - y - z)(1 + \frac{w_dx}{x + y + z}), \quad (30)$$

$$y' = -3[(1 - c_1)y - c_2x] + 3y(2 - x - y - z)(1 + \frac{w_dx}{x + y + z}), \quad (31)$$

$$z' = -3z[1 - (2 - x - y - z)(1 + \frac{w_dx}{x + y + z})]. \quad (32)$$

The corresponding critical points (x_*, y_*, z_*) of the autonomous system (30)-(32) are obtained as follows:

- **Point A:** $(-\frac{c_1-c_2-w_d-x_s}{2w_d}, -\frac{c_1-c_2+w_d-x_s}{2w_d}, 0)$,

- **Point B:** $(-\frac{c_1 - c_2 - w_d + x_*}{2w_d}, -\frac{c_1 - c_2 + w_d + x_*}{2w_d}, 0),$

- **Point C:** $(0, 0, 1).$

In order to study the stability of the critical points for the autonomous system (30)-(32), we obtain the following evolution equations of the linear perturbations:

$$\begin{aligned} \delta x' &= -3[-1 + c_2 + w_d + 2x_* + y_* + z_* + \frac{w_d x_*^2}{x_* + y_* + z_*} - \frac{w_d x_* (2 - x_* - y_* - z_*)(x_* + 2y_* + 2z_*)}{(x_* + y_* + z_*)^2}] \delta x \\ &\quad - 3[c_1 + x_* + \frac{2w_d x_*^2}{(x_* + y_* + z_*)^2}] \delta y - 3x_* [1 + \frac{2w_d x_*}{(x_* + y_* + z_*)^2}] \delta z, \end{aligned} \quad (33)$$

$$\begin{aligned} \delta y' &= 3[c_2 - (1 + w_d)y_* + \frac{2w_d y_*(y_* + z_*)}{(x_* + y_* + z_*)^2}] \delta x \\ &\quad + 3[1 + c_1 - (1 + w_d)x_* - 2y_* - z_* + \frac{2w_d x_*(x_* + z_*)}{(x_* + y_* + z_*)^2}] \delta y - 3y_* [1 + \frac{2w_d x_*}{(x_* + y_* + z_*)^2}] \delta z, \end{aligned} \quad (34)$$

$$\begin{aligned} \delta z' &= -3z_* [1 + w_d - \frac{2w_d(y_* + z_*)}{(x_* + y_* + z_*)^2}] \delta x \\ &\quad - 3z_* [1 + \frac{2w_d x_*}{(x_* + y_* + z_*)^2}] \delta y - 3[-1 + (1 + w_d)x_* + y_* + 2z_* - \frac{2w_d x_*(x_* + y_*)}{(x_* + y_* + z_*)^2}] \delta z. \end{aligned} \quad (35)$$

The corresponding three eigenvalues of the coefficient matrix of Eqs.(33)-(35) are listed in Table II. It is easy to examine that point A is not a stable point, while point B is stable if $w_d > -1, 0 < c_1 < -w_d, 0 < c_2 < c_1 - w_d - 2\sqrt{-w_d c_1}$ or $w_d < -1, 0 < c_1 < -1/w_d, (1 + w_d)(c_1 - 1) < c_2 < c_1 - w_d - 2\sqrt{-w_d c_1}$. We find that for the case of $w > -1$, the stable regions of parameters in LQC are the same as those in classical Einstein cosmology. Additionally, at point B, the accelerated condition $w < -1/3$ can be expressed as

$$\left\{ \begin{array}{lll} 0 < c_1 < -w_d, & 0 < c_2 < (1 + w_d)c_1 - w_d + 1/3 & \text{if } w_d > -1/3; \\ w_d + 2/3 < c_1 < -1/(9w_d), & 0 < c_2 < (1 + w_d)c_1 - w_d + 1/3 & \text{if } -2/3 < w_d < -1/3; \\ 0 < c_1 < -1/(9w_d), & 0 < c_2 < (1 + 3w_d)c_1 - w_d + 1/3 & \text{if } -1 < w_d < -2/3; \\ -1/(9w_d) < c_1 < -w_d, & 0 < c_2 < c_1 - w_d - 2\sqrt{-w_d c_1} & \text{if } -1 < w_d < -1/3; \\ -1/(9w_d) < c_1 < -1/(3w_d), & (1 + w_d)(c_1 - 1) < c_2 < c_1 - w_d - 2/3 & \text{if } w_d < -1; \\ 0 < c_1 < -1/(9w_d), & (1 + w_d)(c_1 - 1) < c_2 < (1 + 3w_d)c_1 - w_d + 1/3 & \text{if } w_d < -1 \end{array} \right. \quad (36)$$

so that point B is an accelerated scaling attractor for any case above, which provides a possibility to alleviate the coincidence problem. It should be noted that point C is stable for the same condition as the case in the classical Einstein cosmology, and therefore, we will neglect discussing this point in the section V.

IV. INTERACTING DARK ENERGY MODEL II

In this section, we study the interaction dark energy model with a constant transfer rate: $Q = \Gamma \rho_m$ [32], which has been used in reheating [33], dark matter decay [34], curvaton decay [35] and the decay of superheavy dark matter particles to a quintessence scalar field [36].

In order to study the dynamical evolution, we additionally define a new dimensionless variable as

$$v \equiv \frac{H_0}{H}, \quad (37)$$

where H_0 denotes the current value of the Hubble parameter, and for convenience, we introduce the parameter

$$\beta = \frac{\Gamma}{H_0}. \quad (38)$$

Point	(x_*, y_*, z_*, v_*)	Eigenvalues	w_*
A	$(0, y_*, 1 - y_*, 0)$	$\lambda_1 = \lambda_2 = 0,$ $\lambda_3 = \frac{3}{2}, \lambda_4 = -3w_d$	0
B	$(1, 0, 0, 0)$	$\lambda_1 = \lambda_2 = \lambda_3 = 3w_d,$ $\lambda_4 = \frac{3}{2}(1 + w_d),$	w_d
C	$(-\frac{1}{w_d}, \frac{1+w_d}{w_d}, 0, \frac{3}{\beta})$	$\lambda_1 = \lambda_2 = -3,$ $\lambda_{3,4} = \frac{3}{2}(-1 - w_d \pm \sqrt{w_d^2 - 1})$	-1

TABLE III: The properties of the critical points for the interacting model II in classical Einstein cosmology.

A. Cosmological Dynamics in Classical Einstein Cosmology

In classical Einstein cosmology, using Eqs.(2)-(6), (37) and (38), we concretely express the autonomous system (11)-(13) as

$$x' = -3w_d x(1 - x) - \beta v y, \quad (39)$$

$$y' = -3w_d x y + \beta v y, \quad (40)$$

$$z' = 3w_d x z, \quad (41)$$

$$v' = \frac{3}{2}v(1 + w_d x), \quad (42)$$

which has three critical points as follows:

- **Point A:** $(0, y_*, 1 - y_*, 0)$,
- **Point B:** $(1, 0, 0, 0)$,
- **Point C:** $(-\frac{1}{w_d}, \frac{1+w_d}{w_d}, 0, \frac{3}{\beta})$.

Substituting linear perturbations $x \rightarrow x_* + \delta x$, $y \rightarrow y_* + \delta y$, $z \rightarrow z_* + \delta z$ and $v \rightarrow v_* + \delta v$ about the critical points into the autonomous system Eqs.(39)-(42), to first-order in the perturbations, we get the following evolution equations of the linear perturbations:

$$\delta x' = -3w_d(1 - 2x_*)\delta x - \beta v_* \delta y - \beta y_* \delta v, \quad (43)$$

$$\delta y' = 3w_d y_* \delta x + (3w_d x_* + \beta v_*)\delta y + \beta y_* \delta v, \quad (44)$$

$$\delta z' = 3w_d z_* \delta x + 3w_d x_* \delta z, \quad (45)$$

$$\delta v' = \frac{3}{2}w_d v_* \delta x + \frac{3}{2}(1 + w_d x_*)\delta v. \quad (46)$$

The four eigenvalues of the coefficient matrix of the above equations determine the stability of the critical points. In Table III, we list the eigenvalues for each point. Then, it is clear that the critical points A and C are not stable if they exist, while point B is stable when $w_d < -1$. Since the total EoS at point B is $w_* = w_d$, point B is an accelerated attractor. Note that it is a dark energy dominated solution, rather than a scaling solution. Thus, this kind of interacting model in classical Einstein cosmology can not be regarded as a candidate to alleviate the coincidence problem.

Point	(x_*, y_*, z_*, v_*)	Eigenvalues	w_*
A	$(0, y_*, 1 - y_*, 0)$	$\lambda_1 = 0, \lambda_2 = -3$ $\lambda_3 = \frac{3}{2}, \lambda_4 = -3w_d$	0
B	$(1, 0, 0, 0)$	$\lambda_1 = \lambda_2 = 3w_d,$ $\lambda_3 = \frac{3}{2}(1 + w_d), \lambda_4 = -3(1 + w_d),$	w_d
C	$(x_*, -(1 + w_d)x_*, 0, \frac{3}{\beta})$	$\lambda_1 = 0, \lambda_2 = \frac{3(w_d+2)}{w_d}$ $\lambda_{3,4} = \frac{3}{2}\{-1 - w_d \pm \sqrt{(1 + w_d)[-3 + w_d(1 - 2x_*)]}\}$	-1

TABLE IV: The properties of the critical points for the interacting model II in LQC.

B. Cosmological Dynamics in LQC

In LQC, inserting Eqs.(37)and (38) into the evolution equations (19)-(21) and making use of Eqs.(14) and (15), we get the autonomous system

$$x' = -3(1 + w_d)x - \beta v y + 3x(2 - x - y - z)(1 + \frac{w_d x}{x + y + z}), \quad (47)$$

$$y' = -3y + \beta v y + 3y(2 - x - y - z)(1 + \frac{w_d x}{x + y + z}), \quad (48)$$

$$z' = -3z[1 - (2 - x - y - z)(1 + \frac{w_d x}{x + y + z})], \quad (49)$$

$$v' = \frac{3}{2}v(2 - x - y - z)(1 + \frac{w_d x}{x + y + z}). \quad (50)$$

The critical points of the autonomous system (47)-(50) is obtained as

- **Point A:** $(0, y_*, 1 - y_*, 0)$,
- **Point B:** $(1, 0, 0, 0)$,
- **Point C:** $(x_*, -(1 + w_d)x_*, 0, \frac{3}{\beta})$.

In order to study the stability of the critical points for the autonomous system (47)-(50), we obtain the following evolution equations of the linear perturbations:

$$\begin{aligned} \delta x' &= -3[-1 + w_d + 2x_* + y_* + z_* + \frac{w_d x_*^2}{x_* + y_* + z_*} - \frac{w_d x_*(2 - x_* - y_* - z_*)(x_* + 2y_* + 2z_*)}{(x_* + y_* + z_*)^2}] \delta x \\ &\quad - \{\beta v_* + 3x_*[1 + \frac{2w_d x_*}{(x_* + y_* + z_*)^2}]\} \delta y - 3x_*[1 + \frac{2w_d x_*}{(x_* + y_* + z_*)^2}] \delta z - \beta y_* \delta v, \end{aligned} \quad (51)$$

$$\begin{aligned} \delta y' &= -3y_*[1 + w_d - \frac{2w_d(y_* + z_*)}{(x_* + y_* + z_*)^2}] \delta x \\ &\quad + \{\beta v_* + 3[1 - (1 + w_d)x_* - 2y_* - z_* + \frac{2w_d x_*(x_* + z_*)}{(x_* + y_* + z_*)^2}]\} \delta y - 3y_*[1 + \frac{2w_d x_*}{(x_* + y_* + z_*)^2}] \delta z + \beta y_* \delta v, \end{aligned} \quad (52)$$

$$\begin{aligned} \delta z' &= -3z_*[1 + w_d - \frac{2w_d(y_* + z_*)}{(x_* + y_* + z_*)^2}] \delta x \\ &\quad - 3z_*[1 + \frac{2w_d x_*}{(x_* + y_* + z_*)^2}] \delta y - 3[-1 + (1 + w_d)x_* + y_* + 2z_* - \frac{2w_d x_*(x_* + y_*)}{(x_* + y_* + z_*)^2}] \delta z, \end{aligned} \quad (53)$$

$$\begin{aligned} \delta v' &= -\frac{3}{2}v_*[1 + w_d - \frac{2w_d(y_* + z_*)}{(x_* + y_* + z_*)^2}] \delta x \\ &\quad - \frac{3}{2}v_*[1 + \frac{2w_d x_*}{(x_* + y_* + z_*)^2}] \delta y - \frac{3}{2}v_*[1 + \frac{2w_d x_*}{(x_* + y_* + z_*)^2}] \delta z + \frac{3}{2}(2 - x - y - z)(1 + \frac{w_d x}{x + y + z}) \delta v. \end{aligned} \quad (54)$$

Solving the four eigenvalues of the coefficient matrix of the above equations, we list them in Table IV. It is not difficult to see that the critical point A is not stable. For point C, to guarantee the energy densities of dark sectors to be positive, we get $w_d < -1$, and therefore the real parts of the eigenvalues λ_3 and λ_4 are positive. This means that point C is not stable. The critical point B is also not stable, since the sign of λ_3 is always opposite to the sign of λ_4 . However, in classical Einstein cosmology point B is stable when $w_d < -1$.

V. NUMERICAL RESULTS

In what follows, we numerically study the dynamical results of the interacting dark energy models to confirm the complicated stability condition for the critical points in both interacting models.

A. The Interacting Model I

In the former model, there are two attractors in both classical Einstein cosmology and LQC. One is a baryon dominated solution which is neglected, and the other is an accelerated scaling solution. Numerical results for the interacting model I are shown in Figs.1-8.

In Fig.1, we depict the parameter space (c_1, c_2) to be stable by choosing $w_d = -0.6$ and $w_d = -1.4$. When $w_d > -1$, the stable region in LQC is the same as that in classical Einstein cosmology, i.e., the critical point B is stable in the region I in both kinds of cosmology. However, when $w_d < -1$, point B is stable in the region I+II in classical Einstein cosmology, whereas in LQC, point B is an attractor only in the region II.

In Fig.2, we plot the phase space trajectories of the universe with w_d , c_1 and c_2 in the stable region. We find that the position of the critical point B depends on the EoS w_d and the coupling constants c_1 and c_2 , but is independent of the theory describing our universe. However, the trajectories in the phase space depend not only upon w_d , c_1 and c_2 , but also upon the selected theory.

Fig.3 shows the evolution of the total EoS w with the chosen parameters w_d , c_1 and c_2 , satisfying the acceleration conditions (29) and (36). Apparently, we can see that in the final state the total EoS w tends to a constant, which depends on w_d , c_1 and c_2 , but is independent of the theory describing our universe.

Fig.4 exhibits the trajectories of scalar factor a versus time for different values of parameters in LQC. We set $\kappa^2 = 1$, and thus take $\rho_c = 1$ since the value of ρ_c is on the order of the Plank density, κ^{-4} . From the figure, one can see that the evolution trajectories are significantly different for varied parameters. The bounce in scale factor occurs later for greater value of w_d , c_1 or c_2 . Our universe finally enters an oscillating phase in LQC.

In Figs.5-8, we plot the evolution trajectories of the Hubble parameter H and energy density ρ versus time. The parameters we selected is in the unstable region in LQC. Differentiating Eq.(14) with respect to ρ , we find that H has a extremum value ($dH/d\rho = 0$) when $\rho = \rho_c/2$. Additionally, the second order derivative of H reads

$$\left(\frac{d^2 H}{d\rho^2}\right)_{\rho=\rho_c/2} = -\frac{2\kappa}{\sqrt{3\rho_c^3}} < 0 \quad (H > 0), \quad (55)$$

$$\left(\frac{d^2 H}{d\rho^2}\right)_{\rho=\rho_c/2} = \frac{2\kappa}{\sqrt{3\rho_c^3}} > 0 \quad (H < 0). \quad (56)$$

Thus, $H_{max} = \sqrt{\kappa^2 \rho_c / 12}$ when $H > 0$, while $H_{min} = -\sqrt{\kappa^2 \rho_c / 12}$ when $H < 0$. In Figs.5-8, with $\rho_c = 1$, a calculation gives $H_{max,min} \approx \pm 0.2887$ at $\rho = \rho_c/2$. When $H \approx 0$, we have the density $\rho \approx \rho_c$ and thus the bounce occurs. From the figures, we find that the expansion of our universe halts at the time when $H \approx 0$, and then contracts until $H \approx 0$ again. The universe goes on bouncing forward and backward. It is worthwhile to note that the oscillating frequencies of $H(t)$ and $\rho(t)$ depend upon the chosen coupling constants c_1 , c_2 and EoS w_d .

B. The Interacting Model II

In the latter model, the dark energy dominated solution is the only attractor solution in classical Einstein cosmology, whereas there exists no attractor in LQC. Numerical results for the interacting model II are presented in Figs.9-14. Since observations constrain the interaction to be sub-dominant today, which indicates $|\Gamma| \ll H_0$, we select the parameter β to be very small in the following numerical analysis.

In Fig.9, we plot three-dimensional phase space trajectories of the universe with $w_d = -1.2$ in the stable region in classical Einstein cosmology. From the figure, we see that the trajectory curves from different initial conditions are converged at a point, the position of which is independent of any parameters.

In Fig.10, the evolution of the total EoS w is plotted. It is easy to see that in the final state w tends to a constant, which equals to w_d . It is worth noting that the evolution trajectory of w is not only independent of the theory describing our universe but also independent of the coupling constant β . In other words, the coupling constant do not affect the evolution result.

Fig.11 show the trajectories of scalar factor a versus time for different values of parameters in LQC. We also take $\kappa^2 = 1$ and $\rho_c = 1$. The evolution trajectories for different values of parameters are distinct. The bounce in scale factor occurs later for greater value of w_d or β . Our universe finally enters an oscillating phase in LQC.

In Figs.12-14, we plot the evolution trajectories of the Hubble parameter H and energy density ρ versus time. The parameters we selected as those above is in the unstable region in LQC. The universe goes on bouncing forward and backward. The oscillating frequencies of $H(t)$ and $\rho(t)$ depend not only upon EoS w_d but also upon the coupling constant β .

VI. CONCLUSIONS

In previous sections, we have studied the cosmological evolution of two interacting dark energy models in classical Einstein and Loop Quantum Cosmology. We consider two kinds of interaction term between dark energy and cold dark matter. Note that observations at the level of the solar system severely constrain non-gravitational interactions of baryons. So the baryonic matter solely satisfies the energy conservation equation. By our analysis, we find that dynamical results in LQC are different from those in classical Einstein cosmology for both two kinds of interacting models.

In the interacting model I, namely, $Q = 3H(c_1\rho_m + c_2\rho_d)$, there are two attractors in both classical Einstein cosmology and LQC. One is a baryon dominated solution and the other is an accelerated scaling solution. Since the same results are obtained in both classical Einstein cosmology and LQC for the baryon dominated attractor, we only focus on the accelerated scaling solution. Interestingly, we find that if $w_d > -1$, the stable region in LQC is the same as that in classical Einstein cosmology, while when $w_d < -1$, the stable region in LQC is smaller than that in classical Einstein cosmology. The total EoS w approaches finally to a constant, which depends on EoS w_d and the coupling constants c_1 and c_2 , but is independent of the theory describing our universe. When we select the parameters in the unstable region in LQC, the universe experience bouncing, which can resolve the singularity problem. The bounce in scale factor occurs later for greater value of w_d , c_1 or c_2 . Furthermore, the oscillating frequencies are distinct for different parameters.

However, in the interacting model II with $Q = \Gamma\rho_m$, there exists one attractor in classical Einstein cosmology for $w_d < -1$, which is a dark energy dominated solution rather than a scaling solution, whereas in LQC, all fixed points is not stable. Thus, there exists no scaling solutions in the interacting model II. So this kind of interacting dark energy model can not be regarded as a candidate to alleviate the coincidence problem in both classical Einstein and loop quantum cosmology. In classical Einstein cosmology, the final state w_* is a constant, which equals to w_d and is independent of the coupling constant β . The bounce in scale factor occurs later for greater value of w_d or β . Our universe finally enters an oscillating phase in LQC. Moreover, the oscillating frequencies are significantly different for varied parameters.

In summary, the interacting model I may alleviate the coincidence problem in both classical Einstein and loop quantum cosmology, depending on the values of the parameters selected in the model. However, the interacting model II can not be regarded as a candidate to alleviate the coincidence problem in both kinds of cosmology. Thus, dynamical results are different not only in different theories describing the universe but also in different interacting models. In addition, the results that our universe finally enters an oscillating phase in LQC, which are different from the those obtained in classical Einstein cosmology, show that LQC allow us the possibility of resolving future singularities. Therefore, the quantum gravity effect may be manifested in large scale in the interacting dark energy models.

Acknowledgements

This work is a part of projects 10675019 and 10975017 supported by NSFC.

-
- [1] A.G. Riess et al., *Astrophys. J.* **116**, 1009 (1998); S. Perlmutter et al., *Astrophys. J.* **517**, 565 (1999); J.L. Tonry et al., *Astrophys. J.* **594**, 1 (2003); R.A. Knop et al., *Astrophys. J.* **598**, 102 (2003).

- [2] S. Masi et al., Prog. Part. Nucl. Phys. **48**, 243 (2002); D. N. Spergel et al., Astrophys. J. Suppl. **148**, 175 (2003); C. L. Bennett et al., Astrophys. J. Suppl. **148**, 1 (2003).
- [3] M. Tegmark et al., Phys. Rev. D **69**, 103501 (2004); K. Abazajian et al., Astrophys. J. **128**, 502 (2004); U. Seljak et al., Phys. Rev. D **71**, 103515 (2005).
- [4] V. Sahni and A. Starobinsky, Int. J. Mod. Phys. D **9**, 373 (2000); S.M. Carroll, Living Rev. Rel. **4**, 1 (2001); P.J.E. Peebles and B. Ratra, Rev. Mod. Phys. **75**, 559 (2003); E.J. Copeland, M. Sami and S. Tsujikawa, Int. J. Mod. Phys. D **15**, 1753 (2006).
- [5] B. Ratra and P.J.E. Peebles, Phys. Rev. D **37**, 3406 (1988); P.J.E. Peebles and B. Ratra, Astrophys. J. **325**, L17 (1988); J.P. Ostriker and P.J. Steinhardt, Nature **377**, 600 (1995); S.M. Carroll, Phys. Rev. Lett. **81**, 3067 (1998); R.R. Caldwell, R. Dave and P.J. Steinhardt, Phys. Rev. Lett. **80**, 1582 (1998); N.A. Bahcall, J.P. Ostriker, S. Perlmutter and P.J. Steinhardt, Science **284**, 1481 (1999); I. Zlatev, L. Wang and P.J. Steinhardt, Phys. Rev. Lett. **82**, 896 (1999); V. Sahni, Class. Quant. Grav. **19**, 3435 (2002).
- [6] R.R. Caldwell, Phys. Lett. B **545**, 23 (2002); R.R. Caldwell, M. Kamionkowski, N.N. Weinberg, Phys. Rev. Lett. **91**, 071301 (2003); P. Singh, M. Sami, N. Dadhich, Phys. Rev. D **68**, 023522 (2003); E. Elizalde, S. Nojiri and S.D. Odintsov, Phys. Rev. D **70**, 043539 (2004).
- [7] A. Sen, JHEP **0207**, 065 (2002); T. Padmanabhan, Phys. Rev. D **66**, 021301 (2002); T. Padmanabhan and T.R. Choudhury, Phys. Rev. D **66**, 081301 (2002).
- [8] B. Feng, X.L. Wang and X.M. Zhang, Phys. Lett. B **607**, 35 (2005); Z.K. Guo, Y.S. Pia, X.M. Zhang and Y.Z. Zhang, Phys. Lett. B **608**, 177 (2005); X. Zhang, Commun. Theor. Phys. **44**, 762 (2005).
- [9] N. Arkani-Hamed, P. Creminelli, S. Mukohyama and M. Zaldarriaga, JCAP **0404**, 001 (2004); F. Piazza and S. Tsujikawa, JCAP **0407**, 004 (2004).
- [10] A.Y. Kamenshchik, U. Moschella and V. Pasquier, Phys. Lett. B **511**, 265 (2001); M.C. Bento, O. Bertolami and A.A. Sen, Phys. Rev. D **66**, 043507 (2002); M.C. Bento, O. Bertolami and A.A. Sen, Phys. Rev. D **70**, 083519 (2004).
- [11] C. Csaki, M. Graesser, L. Randall and J. Terning, Phys. Rev. D **62**, 045015 (2000).
- [12] L. Qiang, Y. Ma, M. Han and D. Yu, Phys. Rev. D **71**, 061501 (2005).
- [13] L.P. Chimento, A.S. Jakubi, D. Pavon and W. Zimdahl, Phys. Rev. D **67**, 083513 (2003); Z.K. Guo, R.G. cai and Y.Z. Zhang, JCAP **0505**, 002 (2005); L.P. Chimento and D. Pavon, Phys. Rev. D **73**, 063511 (2006).
- [14] C.M. Will, Living Rev. Rel. **4**, 4 (2001).
- [15] T. Thiemann, Modern Canonical Quantum General Relativity, Cambridge University, Press, 2007; A. Ashtekar and J. Lewandowski, Class. Quant. Grav. **21**, R53 (2004); M. Han, Y. Ma, W. Huang, Int. J. Mod. Phys. D **16**, 1397 (2007).
- [16] A. Ashtekar, T. Pawlowski and P. Singh, Phys. Rev. Lett. **96**, 141301 (2006); Phys. Rev. D **74**, 084003 (2006).
- [17] P. Singh, Phys. Rev. D **73**, 063508 (2006); E.J. Copeland, J.E. Lidsey and S. Mizuno, Phys. Rev. D **73**, 043503 (2006).
- [18] M. Sami, P. Singh and S. Tsujikawa, Phys. Rev. D **74**, 043514 (2006); T. Cailleteau, A. Cardoso, K. Vandersloot and D. Wands, Phys. Rev. Lett. **101**, 251302 (2008).
- [19] X. Zhang and Y. Ling, JCAP **0708**, 012 (2007).
- [20] Y. Ding, Y. Ma and J. Yang, Phys. Rev. Lett. **102**, 051301 (2009).
- [21] D. Samart and B. Gumjupai, Phys. Rev. D **76**, 243514 (2007).
- [22] B. Gumjupai, *Coupled phantom field in loop quantum cosmology*, arXiv: gr-qc/0706.3467; P.X. Wu, S.N. Zhang, JCAP **06**, 007 (2008).
- [23] H. Wei and S. N. Zhang, Phys. Rev. D **76**, 063005 (2007).
- [24] S.B. Chen, B. Wang and J.L. Jing, Phys. Rev. D **78**, 123503 (2008).
- [25] S.M. Carroll, M. Hoffman and M. Trodden, Phys. Rev. D **68**, 023509 (2003).
- [26] W. Zimdahl, D. Pavon and L.P. Chimento, Phys. Lett. B **521**, 133 (2001); L.P. Chimento, A.S. Jakubi, D. Pavon and W. Zimdahl, Phys. Rev. D **67**, 083513 (2003).
- [27] A. Ashtekar, J. Baez, A. Corichi and K. Krasnov, Phys. Rev. Lett. **80**, 904 (1998); M. Domagala and J. Lewandowski, Class. Quant. Grav. **21**, 5233 (2004); K. A. Meissner, Class. Quant. Grav. **21**, 5245 (2004).
- [28] G. Caldera-Cabral, R. Maartens and L.A. Ureña-López, Phys. Rev. D **79**, 063518 (2009).
- [29] M. Quartin, M.O. Calvao, S.E. Joras, R.R.R. Reis, and I. Waga, JCAP **0805**, 007 (2008).
- [30] H.M. Sadjadi and M. Alimohammadi, Phys. Rev. D **74**, 103007 (2006).
- [31] L. Amendola, Phys. Rev. D **62**, 043511 (2000); W. Zimdahl, Int. J. Mod. Phys. D **14**, 2319 (2005); D. Pavon and W. Zimdahl, Phys. Lett. B **628**, 206 (2005); Z.K. Guo, N. Ohta and S. Tsujikawa, Phys. Rev. D **76**, 023508 (2007); L. Amendola, G.C. Campos, R. Rosenfeld, Phys. Rev. D **75**, 083506 (2007); D. Pavon and B. Wang, Gen. Rel. Grav. **41**, 1 (2009).
- [32] C.G. Boehmer, G. Caldera-Cabral, R. Lazkoz and R. Maartens, Phys. Rev. D **78**, 023505 (2008).
- [33] M.S. Turner, Phys. Rev. D **28**, 1243 (1983).
- [34] R. Cen, Astrophys. J. **546**, L77 (2001); M. Oguri, K. Takahashi, H. Ohno and K. Kotake, Astrophys. J. **597**, 645 (2003).
- [35] K.A. Malik, D. Wands and C. Ungarelli, Phys. Rev. D **67**, 063516 (2003).
- [36] H. Ziaeeepour, Phys. Rev. D **69**, 063512 (2004).

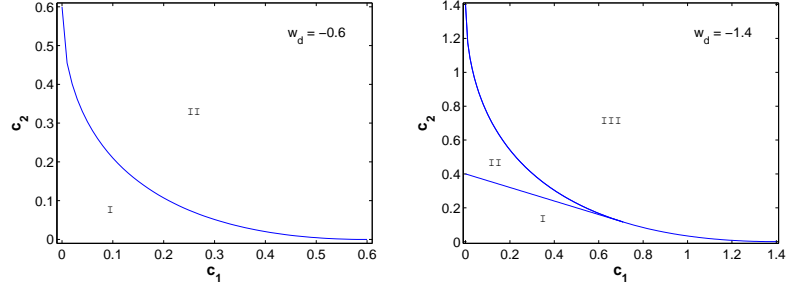


FIG. 1: The stable regions in the (c_1, c_2) parameter space with the fixed w_d for the interacting model I. In the left plot ($w_d > -1$), the critical point B is stable in the region I in classical Einstein cosmology and LQC. In the right plot ($w_d < -1$), point B is stable in the regions I+II in classical Einstein cosmology, whereas in LQC, point B is an attractor only in the region II. The region II in the left and the region III in the right represent the regions of the physically meaningless solution.

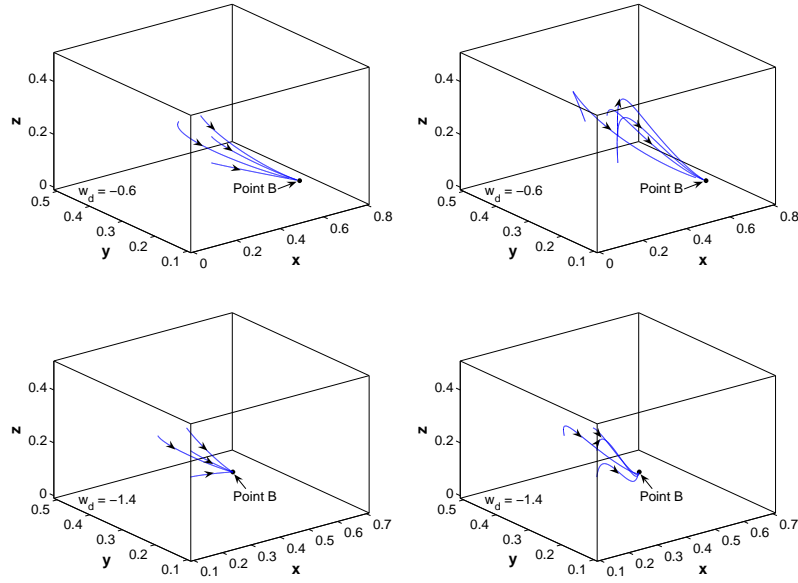


FIG. 2: Three-dimensional phase space of (x, y, z) with the fixed w_d for the interacting model I. The left and right two plots respectively denote classical Einstein cosmology and LQC. In the top two plots, we select the parameters $c_1 = 0.1$ and $c_2 = 0.15$. The bottom two plots is for $c_1 = 0.1$ and $c_2 = 0.5$.

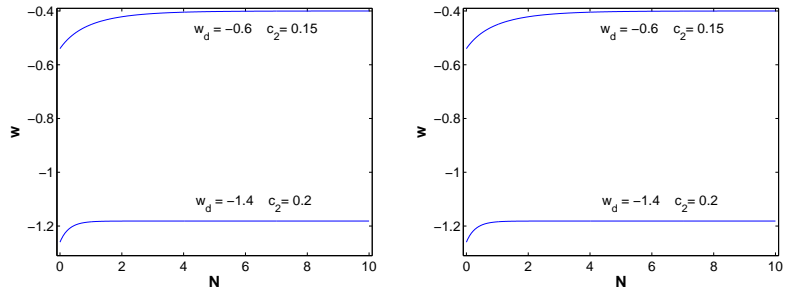


FIG. 3: The evolution of the EoS of total cosmic fluid w with the fixed w_d for the interacting model I. The left is for classical Einstein cosmology and the right is for LQC. The parameter c_1 is chosen as 0.1.

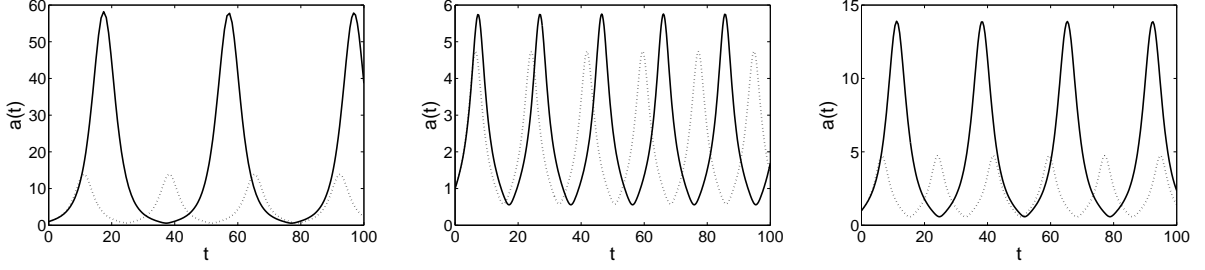


FIG. 4: The plots of scalar factor a as a function of time for the fixed parameters. The left plot is for $w_d = -1.4$ and $c_1 = 0.1$. The solid and dotted lines respectively correspond to $c_2 = 0.2$ and $c_2 = 0.1$. The middle plot is for $w_d = -1.6$ and $c_2 = 0.1$. The solid and dotted lines respectively correspond to $c_1 = 0.3$ and $c_1 = 0.1$. The right plot is for $c_1 = c_2 = 0.1$. The solid and dotted lines respectively correspond to $w_d = -1.4$ and $w_d = -1.6$.

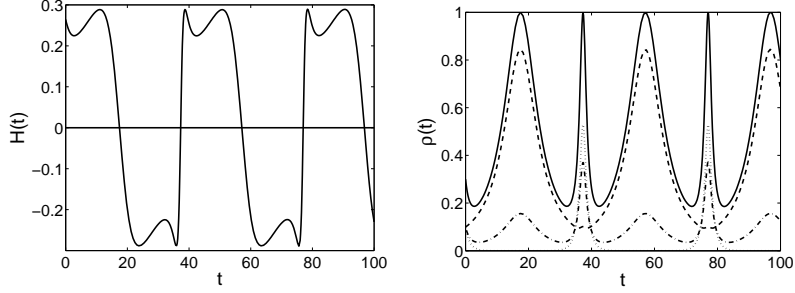


FIG. 5: The evolution of the Hubble parameter H and the energy density ρ with respect to time with $w_d = -1.4$, $c_1 = 0.1$, $c_2 = 0.2$. The solid, dashed, dash-dotted and dotted lines correspond to ρ , ρ_d , ρ_m and ρ_b , respectively.

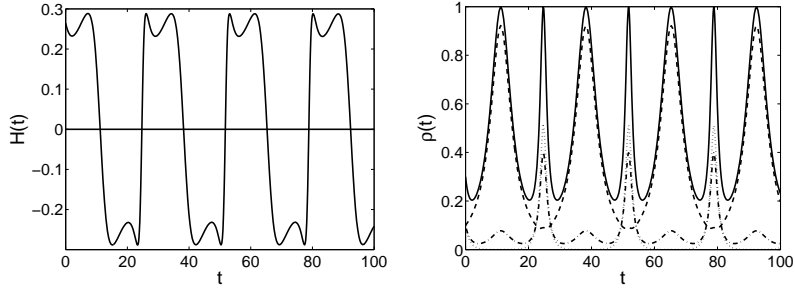


FIG. 6: The evolution of the Hubble parameter H and the energy density ρ with respect to time with $w_d = -1.4$, $c_1 = 0.1$, $c_2 = 0.1$. The solid, dashed, dash-dotted and dotted lines correspond to ρ , ρ_d , ρ_m and ρ_b , respectively.

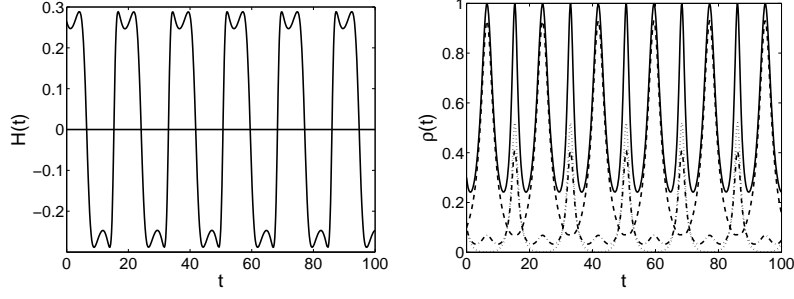


FIG. 7: The evolution of the Hubble parameter H and the energy density ρ with respect to time with $w_d = -1.6$, $c_1 = 0.1$, $c_2 = 0.1$. The solid, dashed, dash-dotted and dotted lines correspond to ρ , ρ_d , ρ_m and ρ_b , respectively.

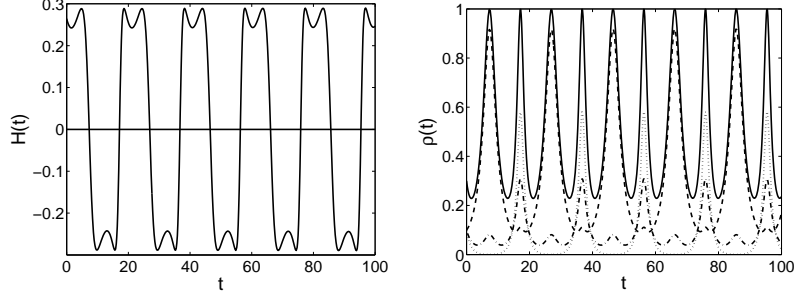


FIG. 8: The evolution of the Hubble parameter H and the energy density ρ with respect to time with $w_d = -1.6$, $c_1 = 0.3$, $c_2 = 0.1$. The solid, dashed, dash-dotted and dotted lines correspond to ρ , ρ_d , ρ_m and ρ_b , respectively.

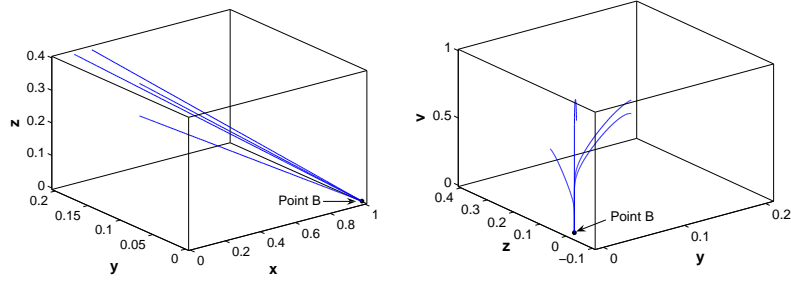


FIG. 9: Three-dimensional phase space for the interacting model II with $w_d = -1.2$ in classical Einstein cosmology. The left is for the phase space of (x, y, z) and the right is for the phase space of (y, z, v) .

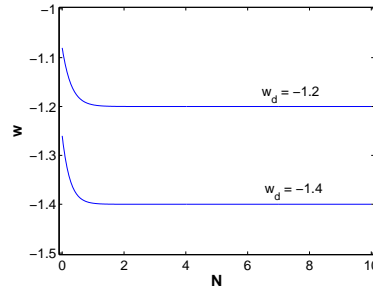


FIG. 10: The evolution of the EoS of total cosmic fluid w for the interacting model II with $\beta = 10^{-6}$ in LQC (the same as in classical Einstein cosmology).

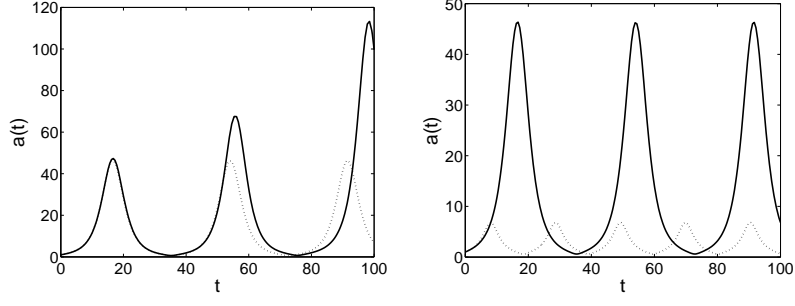


FIG. 11: The plots of scalar factor a as a function of time for the interacting model II. The left plot is for $w_d = -1.2$, in which the solid and dotted lines denote the cases of $\beta = 10^{-2}$ and $\beta = 10^{-6}$, respectively. The right is for $\beta = 10^{-6}$, in which the solid and dotted lines represent $w_d = -1.2$ and $w_d = -1.4$, respectively.

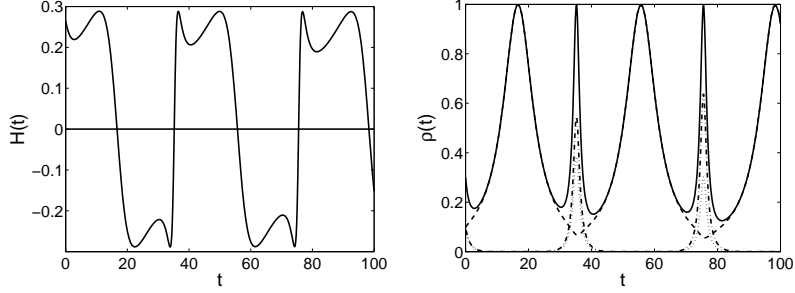


FIG. 12: The evolution of the Hubble parameter H and the energy density ρ with respect to time for $w_d = -1.2, \beta = 10^{-2}$. The solid, dashed, dash-dotted and dotted lines correspond to ρ, ρ_d, ρ_m and ρ_b , respectively.

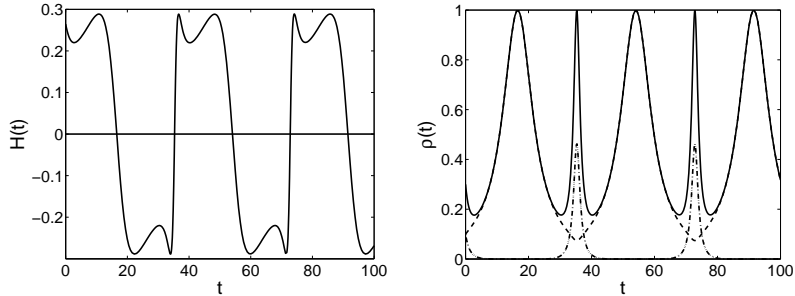


FIG. 13: The evolution of the Hubble parameter H and the energy density ρ with respect to time for $w_d = -1.2, \beta = 10^{-6}$. The solid, dashed, dash-dotted and dotted lines correspond to ρ, ρ_d, ρ_m and ρ_b , respectively.

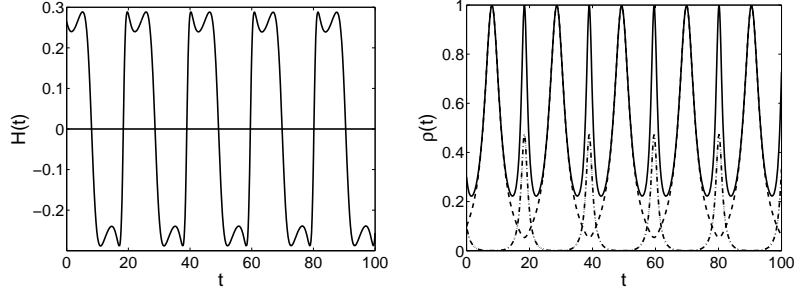


FIG. 14: The evolution of the Hubble parameter H and the energy density ρ with respect to time for $w_d = -1.4, \beta = 10^{-6}$. The solid, dashed, dash-dotted and dotted lines correspond to ρ, ρ_d, ρ_m and ρ_b , respectively.

